SCIENTIFIC ARTICLE

Intermittent Cyclic Mechanical Tension Promotes Degeneration of Endplate Cartilage via the Nuclear Factor-κB Signaling Pathway: an *in Vivo* Study

Liang Xiao, MB, Hong-guang Xu, MD, Hong Wang, BS, Ping Liu, BS, Chen Liu, MM, Xiang Shen, MM, Tao Zhang, MB, Yong-ming Xu, MB

Department of Orthopaedic Surgery, Yijishan Hospital, Wannan Medical College, Wuhu, China

Objective: To establish a rabbit model for investigating the effects of intermittent cyclic mechanical tension (ICMT) on promoting degeneration of endplate cartilage.

Methods: Forty New Zealand white rabbits were subjected to surgery and randomly divided into three equal groups as follows: control group (no treatment, $n = 10$), sham group (animals underwent a sham operation but were not subjected to mechanical tensile strain, $n = 15$) and loaded group (discs were subjected to 1.5 MPa external tensile loading by using an external loading device during the animals' daily activity, $n = 15$). Mechanical tensile strain was applied for 8 h/d. The animals were examined radiologically after 8 weeks treatment and then killed for removal of endplate cartilage tissue samples from their spines. Histological staining was performed to examine the morphology of endplate cartilage tissue. Multiple strategies were employed to examine degeneration of endplate cartilage and nuclear factor (NF)-κB signaling pathway activation.

Results: After ICMT loading for 56 days, radiology revealed ossification, hyperosteogeny and stenosis in the intervertebral spaces. Examination of hematoxylin and eosin staining of sections of endplate cartilage showed significant damage as the load duration increased in the ICMT loading group. Expression of aggrecan (ACAN), type II collagen (COL-2A), SRY-related high mobility group-box gene 9 (SOX9) was down-regulated ($F_{ACAN} = 21.515$, $P < 0.01$; $F_{COL\text{-}2A} = 6.670$, $P = 0.05$; $F_{SOX9} = 7.888$, $P < 0.05$), whereas that of matrix metallopeptidase 13 (MMP13) was up-regulated ($F_{MMP13} = 14.120$, $P < 0.01$) after ICMT. Western blot and immunofluorescence revealed that expression of protein was consistent with gene expression results. Additionally, ICMT loading can lead to NF-κB signaling pathway activation as well as degeneration of endplate cartilage.

Conclusion: These experiments indicate that ICMT contributes to the activation of NF-κB signaling pathway *in vivo* and that the NF-κB signaling pathway further up-regulates MMP13, leading to degeneration of endplate cartilage.

Key words: Endplate cartilage degeneration; *In vivo*; Intermittent cyclic mechanical tension; NF-κF signaling pathway

Introduction

Intervertebral disc degeneration (IDD) is an underlying cause of many chronic debilitating and pathological disorders, including intervertebral disc herniation, spinal stenosis and spine instability[1,2]. Being the gateway for nutrient transport between the vertebral marrow and intervertebral disc, endplate cartilage is closely correlated with IDD[3]. Many studies have showed that degeneration of the cartilaginous endplate plays a key role in the process of IDD. That is, endplate cartilage damage and loss of the chondrogenic phenotype increase the risk of internal disruption in discs, which promotes disc degeneration[4,5].

In the human body, mechanical stimulation is the outcome of co-application of pressure and tension. Being the part

Address for correspondence Hong-guang Xu, MD, Department of Orthopaedic Surgery, Yijishan Hospital, Wannan Medical College, 2 West Zheshan Street, Wuhu, Anhui, China 241001 Tel: 0086-013855356303; Fax: 0086-553-5739037; Email: xlllan2012@126.com

Disclosure: This study was supported by the Chinese National Natural Science Foundation Project (Grant Nos. 81272048 and 81572185).
Received 5 April 2016; accepted 28 June 2016

of the joint that bears loading, the endplate cartilages are exposed to a combination of mechanical stress in which tensile strain plays a critical role[6,7]. Many studies have demonstrated that low magnitude and low frequency tensile strain has an anti-inflammatory function, promoting cartilaginous gene expression and matrix synthesis. In contrast, high magnitude and high frequency tensile strain inhibits anabolism and induces both catabolism and expression of inflammatory factors in chondrocytes[8–10]. Our previous study showed that intermittent cyclic mechanical tension (ICMT) induces endplate chondrocyte calcification and decreases expression of chondrocyte anabolic genes such as type II collagen (COL-2A), aggrecan (ACAN) and SRY-related high mobility group-box gene 9 (Sox9)[11,12]. However, the mechanisms by which biomechanical factors such as tension regulate metabolism in endplate cartilage are still not well understood.

Nuclear factor (NF)-κB is a family of transcription factors that play a central role in mediating cellular responses to damage, stress and inflammation. Various proinflammatory cytokines and mediators, such as tumor necrosis factor-α, interleukin-1 and -6, have been shown to be regulated by NF-κB[13]. The mammalian NF-κB family consists of five subunits, the most common and abundant form being the p50/p65 heterodimer. In its inactive form, NF-κB is located in the cytosol, coupled to the inhibitory molecule, IκB. Activation signals can result in IκB dissociating from the NF-κB complex. This allows phosphorylated p50/p65 to translocate from the cytosol to the nucleus and bind to specific DNA sequences to initiate transcription[14]. The role of NF-κB signaling in degeneration of endplate cartilage is far less clear; however, there is some evidence that it is involved in the degeneration of articular cartilage that occurs in osteoarthritis[15–17]. Moreover, some studies have shown that mechanical strain exploits NF-κB as a common pathway for transcriptional inhibition/activation of proinflammatory genes and catabolic processes in chondrocytes[18].

Based on these observations, we hypothesized that activation of NF-κB signaling pathway plays a central role in mediating tension-related degenerative changes in endplate cartilage. In this study, we tested this hypothesis by establishing an *in vivo* rabbit model that responds similarly to humans to mechanical stimulation.

Materials and Methods

Animals

Forty skeletally mature male New Zealand white rabbits (6 months old) weighing an average of 3 kg were used in this study, which was conducted under a protocol approved by the Committee on the Ethics of Animal Experiments of the Yijishan Hospital, Wannan Medical College. All rabbits were randomly assigned to a control (n = 10), sham (n = 15) or loaded group (n = 15). Rabbits in the sham and loaded groups were subjected to general anesthesia and underwent surgery as described previously[19–21].

Surgical Procedure

The rabbits were anesthetized with 10% chloral hydrate administered via the marginal ear vein. Through a dorsal approach to the lumbar spine, an external loading device (Fig. 1A) was attached using four stainless steel pins placed percutaneously and attached to two K-wires (diameter 1 mm) inserted into the L_4 and L_5 vertebral bodies parallel to the adjacent disc by the use of a variable-speed electric drill. After closure of the surgical wound, the discs of the loaded group rabbits were subjected to shear force for 8 h a day, imitating human daily life. A dynamometer was used to create axial tension to the disc so as to produce a calculated pulling force of 1.5 MPa (15 kg/cm^2). In the sham group, the external loading device was put in place but no tension force applied. Animals in the control group served as intact control subjects. After surgery, all animals were allowed free unrestricted activity in standardized cages and monitored according to a standardized protocol (Fig. 1B).

Radiology and Histological Staining

After 56 days of loading, lateral radiographs of each animal were taken, after which they were killed. Their lumbar spines were dissected and the endplate cartilages removed. Lumbar spines from rabbits treated with or without mechanical tensile loading were fixed in 10% paraformaldehyde, decalcified, and embedded in paraffin and the tissue sections were stained with hematoxylin and eosin (H&E).

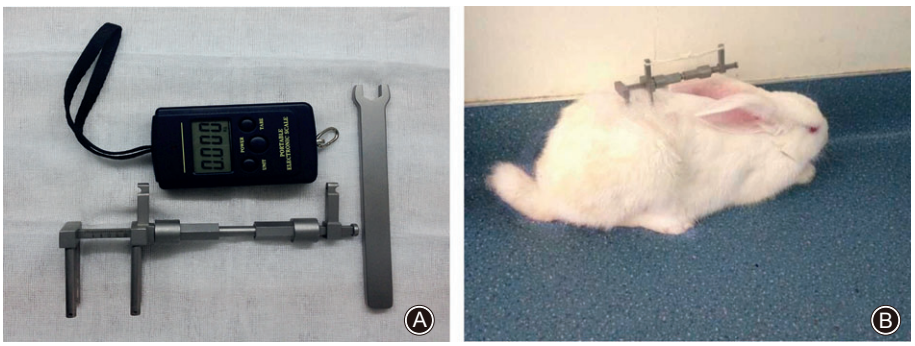

Fig. 1 External loading device and animal model. (A) The loading device can produce and maintain a mechanical tensile strain of 1.5 MPa (Patent number: 201120575941.X). (B) After surgery, the animals were allowed free unrestricted weight-bearing and activity.

Real-Time Reverse-Transcription Polymerase Chain Reaction (RT-PCR)

Total RNA was isolated from endplate cartilage samples using Trizol reagent (Invitrogen, Carlsbad, CA, USA) according to the manufacturer's instructions. After reverse transcription, real-time PCR was performed by a Light-Cycler480 System (Roche, Basel, Switzerland) using SYBR1 Premix Ex Taq (Takara, Dalian, China) according to the manufacturer's instructions. The conditions of real-time PCR were as follows: denaturation at 95 °C for 10 s, 40 cycles at 95 °C for 10 s and 60 °C for 30 s. Dissociation curves revealed no nonspecific amplification. Glyceraldehyde-3-phosphate dehydrogenase (GAPDH) was used as an internal control. Data were analyzed using the Ct $2^{-\Delta\Delta Ct}$ method and expressed as the fold change compared with the control. Each sample was analyzed in triplicate. Primer sequences for the endplate cartilage samples are listed in Table 1.

Western Blot

Total protein was extracted from the tissue in Radio-Immunoprecipitation Assay lysis buffer (containing protease and phosphatase inhibitor mixtures) by using a tissue homogenizer, followed by clearing tissue debris by centrifugation at 13,000 r/min at 4 °C for 20 min. Protein was quantified using a BCA Protein Assay kit (KeyGen Biotech, Nanjing, China) and then heated in sodium dodecyl sulfate-polyacrylamide gels electrophoresis (SDS-PAGE) protein loading buffer at 95 °C for 10 min. Next, proteins (30 μg per lane) were loaded onto a 10% SDS-PAGE for ACAN (250 kDa), COL-2A (150 kDa), MMP13 (54 kDa), IκB (78 kDa), p65 (60 kDa), p-p65 (60 kDa) and GADPH (36 kDa) and subsequently electrotransferred to a polyvinylidene fluoride membrane. After blocking with 5% bovine serum albumin in Tris buffer saline Tween 20 (TBST), the membranes were immunoblotted with rat anti-ACAN, rat anti-COL-2A, rabbit anti-MMP13, rabbit anti-IκB, rabbit anti-p65, rabbit anti-p-p65 and rat anti-GAPDH antibodies (1:1000) overnight at 4 °C. The membranes were then washed three times with TBST and incubated with anti-rat or anti-rabbit horseradish peroxidase-conjugated secondary IgG (1:5000) at room temperature for 1 h. The bound complex was detected using Odyssey Infrared Imaging System (Li-Cor Biosciences, Lincoln, NE, USA). The images were analyzed using Odyssey Application Software, version 1.2 (Li-Cor) to obtain the integrated intensities.

Immunofluorescence

Paraffin sections of endplate cartilage tissue were deparaffinized, dehydrated using graded ethanol, antigen repaired, washed with 0.01 mol/L phosphate-buffered saline with Tween-20, and then blocked with 2% goat serum for 30 min. Tissues were incubated with primary antibodies overnight at 4 °C. Primary antibodies included a rabbit anti-MMP-13 antibody (1:100 dilution). After washing, the tissues were incubated with a goat anti-rabbit fluorescein isothiocyanate secondary antibody (1:500 dilution) for 1 h at room temperature. Finally, the tissues were incubated with 100 μL DAPI for 5 min and then visualized under a confocal microscope (Leica, Heidelberg, Germany).

Statistical Analysis

All quantitative data are expressed as the mean with 95% confidence intervals (*CIs*). Data were obtained from three independent experiments and tested for normality using the Shapiro–Wilk test prior to parametric analyses. For multiple group comparisons, one-way analysis of variance with Tukey's post-hoc test was used. All statistical analyses were conducted with SPSS 18.0 (IBM, Chicago, IL, USA). *P* values of less than 0.05 were considered significant.

Results

Animals

Thirty-nine of the 40 animals survived the complete experiment; one animal did not survive the operation. All animals tolerated the application of the external loading device without postoperative behavioral or neurologic symptoms. Two animals had postoperative infections that were managed by routine surgical dressing changes until the wounds had healed.

Radiographic Analysis

Lateral radiographs showed that the intervertebral spaces in the control group rabbits' lumbar spines were well-proportioned and the vertebral density homogeneous. In the sham group, $L_{4\text{-}5}$ disc heights had decreased and narrowed. In the loaded group, $L_{4\text{-}5}$ intervertebral spaces were stenosed and distinct ossification accompanied by vertebral osteophytes was observed (Fig. 2).

TABLE 1 Sequences of primers used in RT-PCR

Genes	Forward primer	Reverse primer	Product length (bp)
ACAN	3′-ACCCCTGAGGAACAGGAGTT-5′	3′-GTGCCAGATCATCACCACAC-5′	189
COL-2A	3′-GTCTCCATAGCTGAAGTGG-5′	3′-CCATGCAGTACATGCGGG-5′	386
SOX-9	3′-CAGGTGCTCAAGGGTACG-5′	3′-CGGGTGGTCTTTCTTGTGCT-5′	276
MMP13	3′-AACGAGGATGATGATTTGGTCCG	3-5′′-TTGGCCAGGAGGAAAAGCGTGAG-5′	505
GAPDH	3′-GGTGAAGGTCGGAGTGAA-5′	3′-TTCACGCCCATCACAAACA-5′	399

Histological Analysis

Examination of H&E stained sections showed the number and structure of chondrocytes and trabecular bone were regular and clear in the control group. The sham and loaded groups showed degradation of many collagen fibers, this being more pronounced in the latter group. Moreover, many bone trabeculae were developed and disorganized in the loaded group (Fig. 3).

ICMT Promotes Degeneration of Endplate Cartilage in Vivo

There was no significant difference between control and sham groups in expression of ACAN, COL-2A, SOX9 and MMP13 (0.98 ± 0.04 *vs.* 1.00 ± 0.10; 0.92 ± 0.05 *vs.* 1.00 ± 0.16; 0.94 ± 0.05 *vs.* 1.00 ± 0.17; 1.41 ± 0.17 *vs.* 1.00 ± 0.20, respectively; $P > 0.05$). However, ACAN, COL-2A and SOX9 were significantly lower in the loaded group than the control group, by 45% (0.55 ± 0.12 *vs.* 1.00 ± 0.10; $P < 0.01$), 31% (0.69 ± 0.09 *vs.* 1.00 ± 0.16; $P < 0.05$) and 40% (0.60 ± 0.15 *vs.* 1.00 ± 0.17; $P < 0.05$), respectively; whereas MMP13 was significantly greater by 133% (2.33 ± 0.47 *vs.* 1.00 ± 0.20; $P < 0.01$). The results of one-way analysis of variance are listed in Table 2. Western blot also showed down-regulation of expression of COL-2A and ACAN and up-regulation of MMP13 expression in the loaded group compared with the other two groups (Fig. 4A,B). Furthermore, we investigated the level and location of MMP13 by immunofluorescence and found that MMP13 was increased and located in the extracellular matrix (Fig. 4C). These data suggest that endplate chondrocytes lose their phenotype after ICMT loading and that ICMT promotes degeneration of endplate cartilage *in vivo*.

Activation of the NF-κB Signaling Pathway by ICMT in Endplate Cartilage

To investigate the effect of NF-κB signaling on degeneration of endplate cartilage, we used western blotting to detect IκB, p65 and p-p65 expression in rabbit endplate cartilage isolated from three groups. We found that IκB protein was down-regulated in degenerated endplate cartilage. The amount of p65 and p-p65 protein was higher in endplate cartilage in the loaded than in the sham and control groups (Fig. 5). These data suggest activation of NF-κB signaling during degeneration of rabbit endplate cartilage.

Discussion

The intervertebral disc is avascular, disc cells relying mainly on exchange of gas and solutes from the

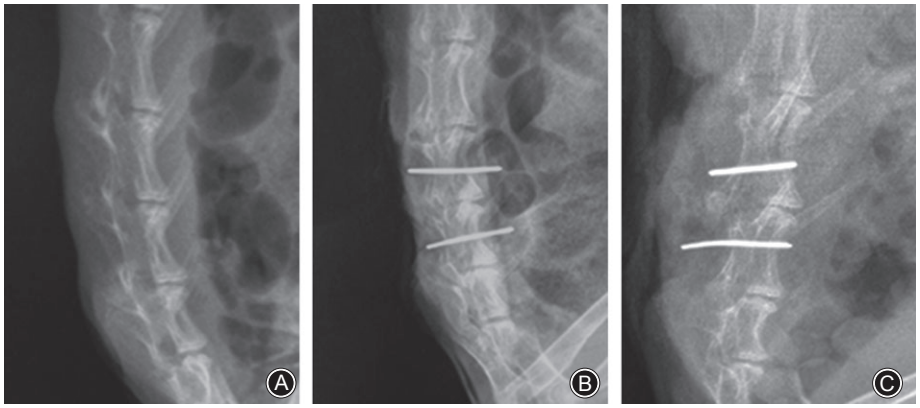

Fig. 2 Examination of lateral radiographs showed that the intervertebral spaces in the lumbar spines in the control group were well-proportioned and the vertebral density homogeneous. In the sham group, the L_{4-5} disc height was decreased and narrowed. In the loaded group, the L_{4-5} intervertebral space was stenosed and distinct ossification accompanied by vertebral osteophytes was observed. (A) Control group. (B) Sham group. (C) Tension-loaded group.

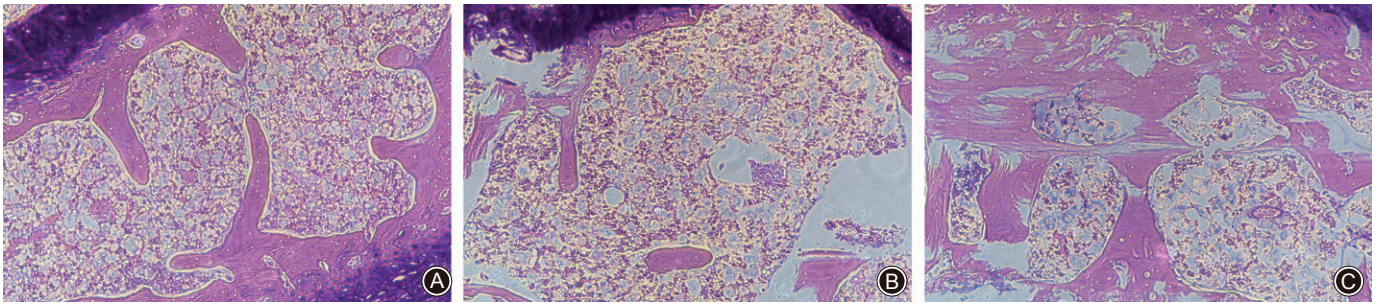

Fig. 3 Examination of H&E stained sections showed endplate cartilage was significantly damaged as the load duration increased in the ICMT loading group. Original magnification: ×40. Representative results from three samples are shown. (A) Control group. (B) Sham group. (C) Loaded group.

TABLE 2 Relative mRNA expression of cartilage genes according to groups (mean ± SD)

Gene	Control group	Sham group	Loaded group	*F* value	*P* value
ACAN	1.00 ± 0.10	0.98 ± 0.04	0.55 ± 0.12*†	21.515	0.002
COL-2A	1.00 ± 0.16	0.92 ± 0.05	0.69 ± 0.09*†	6.670	0.03
SOX9	1.00 ± 0.17	0.94 ± 0.05	0.60 ± 0.15*†	7.888	0.021
MMP13	1.00 ± 0.20	1.41 ± 0.17	2.33 ± 0.47*†	14.120	0.005

*, $P < 0.05$, loaded group versus control group; †, $P < 0.05$, loaded group versus sham group. *P* value by one-way analysis of variance with Tukey honest significance difference test.

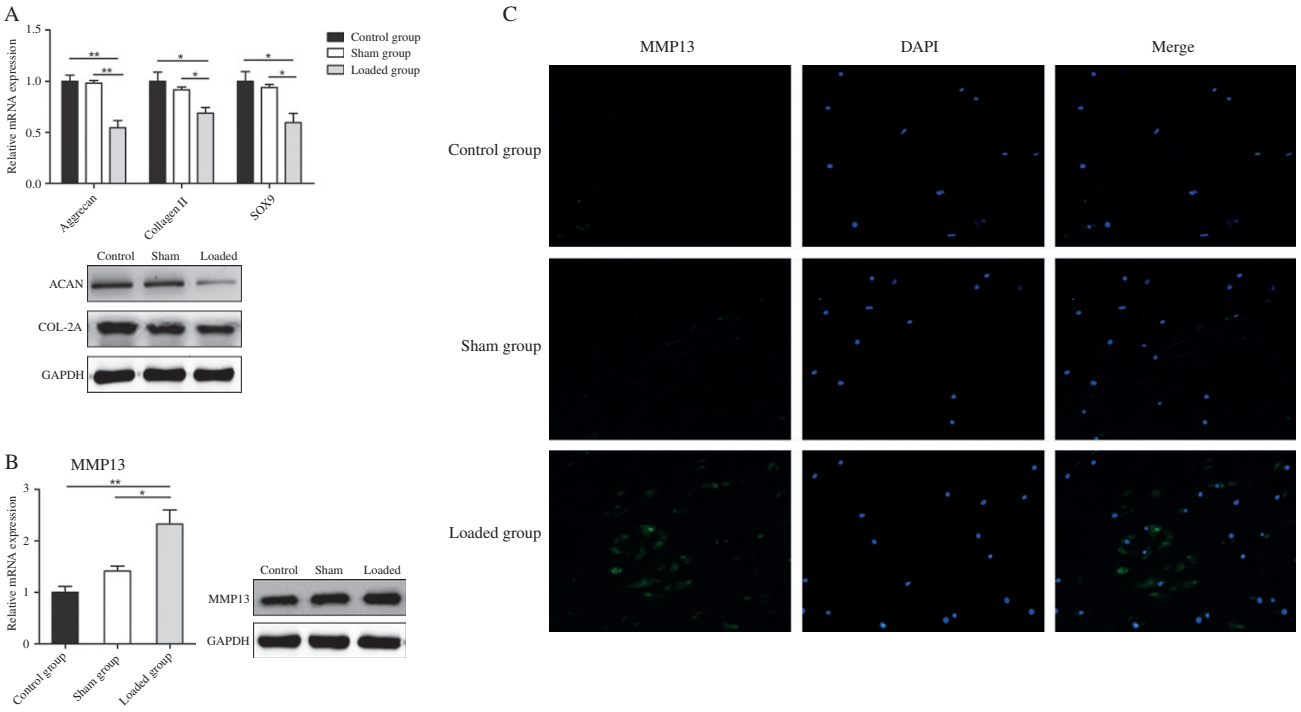

Fig. 4 ICMT induces degeneration of endplate cartilage. (A) Real-time RT-PCR and western blot analyses of COL-2A, ACAN, Sox9 mRNA and protein expression in samples from three groups. Data are presented as mean ± SD, $n \geq 3$/group. All experiments were repeated at least three times. *, $P < 0.05$; **, $P < 0.01$. (B) MMP13 mRNA and protein expression was assessed by real-time RT-PCR and western blot after ICMT application. Data are presented as mean ± SD, $n \geq 3$/group. All experiments were repeated at least three times. *, $P < 0.05$. (C) The expression and location of MMP13 protein were detected by immunofluorescence. Representative results from three donors are shown.

capillaries in adjacent subchondral bone[22]. Mechanical failure or calcification of cartilage endplate can disrupt this transport mechanism, impacting the viability of the disc cells and eventually leading to disc degeneration[23]. Biomechanical stimulation has been implicated as a major factor in degeneration of endplate cartilage. Short-term moderate mechanical loading protects chondrocytes from calcification and increases proteoglycan release, whereas high levels and long durations of mechanical loading induce phenotypic changes in chondrocytes[24,25].

Studies have been conducted in animal models to investigate the relationship between loading and degeneration of endplate cartilage[26,27]. These studies have shown that a hyper-physiological magnitude or frequency of loading can induce morphological changes in endplate cartilage degeneration in animals that resemble the changes in human degenerative endplate cartilage. Although these studies proved that accelerated degeneration of endplate cartilage results from loading conditions of a hyper-physiological magnitude, most of these studies have focused only on axial compression loading. The

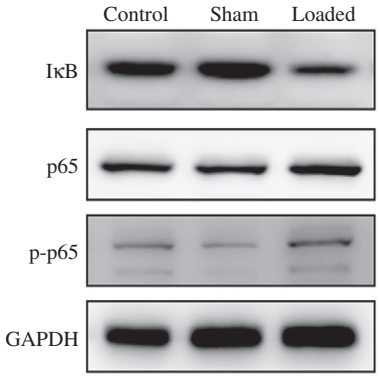

Fig. 5 ICMT promoting activation of NF-κB signaling pathway was assessed by western blotting. IκB expression was down-regulated in the degenerated endplate cartilage, whereas p65 and p-p65 expression was higher in the endplate cartilage of the loaded group than in the sham and control groups.

relationship between degeneration of endplate cartilage and other types of loading has not been thoroughly studied.

Mechanical cervical traction is often recommended for treating patients with neck pain, demonstrating that short-term mechanical cervical traction is beneficial for neck pain. In addition, a recent study showed that shearing stress generated by stepwise stretching plays an important role in inhibiting chondrogenesis[28]. The interface between the endplate and the intervertebral disc is curved; thus, the vertical tension in the interface of endplate in daily life can be decomposed into two forces, one of which is parallel to the endplate and the other perpendicular to it (Fig. 6). These two repetitive stimuli can lead to pathological proliferation and calcification of endplate[29]. Similarly, the present data suggest that excessive intermittent mechanical tensile strain (1.5 MPa, 8 h/d) loading *in vivo* negatively regulates metabolism of the endplate cartilage matrix, ICMT application having induced endplate chondrocyte matrix damage and decreased COL-2A, ACAN, and Sox9 expression in a time-dependent manner. However, the underlying mechanisms for progression of cartilage endplate calcification and degeneration are still not clear.

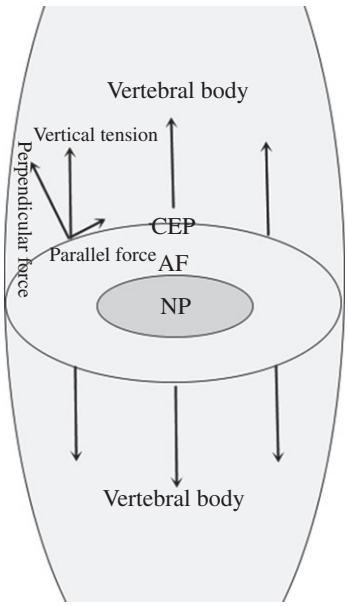

Fig. 6 Tension loading mechanism. Because the interface between the endplate and the intervertebral disc is curved, the erect force is divided into two forces: one of which is parallel and the other perpendicular to the contact face.

MMP13, a collagenase, is a marker of chondrocyte matrix damage and thought to be involved in cartilage calcification[30]. NF-κB signaling in the process of degeneration of cartilage has been well studied[16]. A recent study revealed that NF-κB regulates expression of MMP-1, MMP-3 and MMP-13 genes and proteins in human articular cartilage cells[15]. However, little is yet known about the functions of NF-κB in the endplate cartilage. We hypothesized that the NFkB signaling pathway plays a role in the process of degenerative of endplate cartilage. We found significant activation of the NF-κB signaling pathway in specimens of endplate cartilage from the loaded group. MMP13 protein expression was increased in degenerative endplate cartilage tissues whereas COL-2A and ACAN were decreased. These findings suggest that the effect of MMP13 in degeneration of endplate cartilage may involve activation of the NF-κB pathway.

This study had several limitations. In this article, we first speculated that ICMT increases MMP13 expression through the NF-κB pathway. Unfortunately, their relationship has not been further verified by assessing overexpression or inhibition *in vivo*. Second, ICMT may promote degeneration of endplate cartilage via multiple signaling pathways. However, we only studied NF-κB signaling pathway changes.

In summary, we speculate that ICMT probably activates the NF-κB signaling pathway, thus directly or indirectly targeting MMP13, resulting in degeneration of endplate cartilage. The finding will be useful as a basis for future studies investigating for potentially clinically useful means of attenuating degeneration of endplate cartilage and thus preventing development of IDD.

Acknowledgments

We would like to thank Hong-guang Xu for technical support with the manuscript, Hong Wang, Xiang Shen and Tao Zhang for technical support in performing the *in vivo* experiments, Ping Liu for technical support with radiographic data collection, and Chen Liu for technical support with real time-PCR, western blotting and immunofluorescence analysis.

References

1. Livshits G, Popham M, Malkin I, *et al.* Lumbar disc degeneration and genetic factors are the main risk factors for low back pain in women: the UK twin spine study. Ann Rheum Dis, 2011, 70: 1740–1745.
2. Cheung KM. The relationship between disc degeneration, low back pain, and human pain genetics. Spine J, 2010, 10: 958–960.
3. Malandrino A, Lacroix D, Hellmich C, Ito K, Ferguson SJ, Noailly J. The role of endplate poromechanical properties on the nutrient availability in the intervertebral disc. Osteoarthritis Cartilage, 2014, 22: 1053–1060.
4. Haschtmann D, Stoyanov JV, Gedet P, Ferguson SJ. Vertebral endplate trauma induces disc cell apoptosis and promotes organ degeneration *in vitro*. Eur Spine J, 2008, 17: 289–299.
5. Lama P, Zehra U, Balkovec C, *et al.* Significance of cartilage endplate within herniated disc tissue. Eur Spine J, 2014, 23: 1869–1877.
6. Xu HG, Zhang XH, Wang H, *et al.* Intermittent cyclic mechanical tension-induced calcification and downregulation of ankh gene expression of end plate chondrocytes. Spine (Phila Pa 1976), 2012, 37: 1192–1197.
7. Bleuel J, Zaucke F, Bruggemann GP, Niehoff A. Effects of cyclic tensile strain on chondrocyte metabolism: a systematic review. PLoS One, 2015, 10: e0119816.
8. Xu Z, Buckley MJ, Evans CH, Agarwal S. Cyclic tensile strain acts as an antagonist of IL-1 beta actions in chondrocytes. J Immunol, 2000, 165: 453–460.
9. Honda K, Ohno S, Tanimoto K, *et al.* The effects of high magnitude cyclic tensile load on cartilage matrix metabolism in cultured chondrocytes. Eur J Cell Biol, 2000, 79: 601–609.
10. Kawakita K, Nishiyama T, Fujishiro T, *et al.* Akt phosphorylation in human chondrocytes is regulated by p53R2 in response to mechanical stress. Osteoarthritis Cartilage, 2012, 20: 1603–1609.
11. Xu HG. Autophagy protects endplate chondrocytes from intermittent cyclic mechanical tension induced calcification. Bone, 2015, 75: 242–243.
12. Xu HG, Hu CJ, Wang H, *et al.* Effects of mechanical strain on ANK, ENPP1 and TGF-beta1 expression in rat endplate chondrocytes *in vitro*. Mol Med Rep, 2011, 4: 831–835.
13. Hayden MS, Ghosh S. Shared principles in NF-kappaB signaling. Cell, 2008, 132: 344–362.
14. Hayden MS, West AP, Ghosh S. NF-kappaB and the immune response. Oncogene, 2006, 25: 6758–6780.
15. Lu YC, Jayakumar T, Duann YF, *et al.* Chondroprotective role of sesamol by inhibiting MMPs expression via retaining NF-kappaB signaling in activated SW1353 cells. J Agric Food Chem, 2011, 59: 4969–4978.
16. Pulai JI, Chen H, Im HJ, *et al.* NF-kappa B mediates the stimulation of cytokine and chemokine expression by human articular chondrocytes in response to fibronectin fragments. J Immunol, 2005, 174: 5781–5788.
17. Deschner J, Hofman CR, Piesco NP, Agarwal S. Signal transduction by mechanical strain in chondrocytes. Curr Opin Clin Nutr Metab Care, 2003, 6: 289–293.
18. Agarwal S, Long P, Seyedain A, Piesco N, Shree A, Gassner R. A central role for the nuclear factor-kappaB pathway in anti-inflammatory and proinflammatory actions of mechanical strain. FASEB J, 2003, 17: 899–901.
19. Guehring T, Omlor GW, Lorenz H, *et al.* Stimulation of gene expression and loss of anular architecture caused by experimental disc degeneration—an *in vivo* animal study. Spine (Phila Pa 1976), 2005, 30: 2510–2515.
20. Kroeber MW, Unglaub F, Wang H, *et al.* New in vivo animal model to create intervertebral disc degeneration and to investigate the effects of therapeutic strategies to stimulate disc regeneration. Spine (Phila Pa 1976), 2002, 27: 2684–2690.
21. Guehring T, Nerlich A, Kroeber M, Richter W, Omlor GW. Sensitivity of notochordal disc cells to mechanical loading: an experimental animal study. Eur Spine J, 2010, 19: 113–121.
22. Rodriguez AG, Slichter CK, Acosta FL, *et al.* Human disc nucleus properties and vertebral endplate permeability. Spine (Phila Pa 1976), 2011, 36: 512–520.
23. Jackson AR, Huang CY, Gu WY. Effect of endplate calcification and mechanical deformation on the distribution of glucose in intervertebral disc: a 3D finite element study. Comput Methods Biomech Biomed Engin, 2011, 14: 195–204.
24. Xu H, Zhang X, Wang H, Zhang Y, Shi Y, Zhang X. Continuous cyclic mechanical tension increases ank expression in endplate chondrocytes through the TGF-beta1 and p38 pathway. Eur J Histochem, 2013, 57: e28.
25. Rosenzweig DH, Quinn TM, Haglund L. Low-frequency high-magnitude mechanical strain of articular chondrocytes activates p38 MAPK and induces phenotypic changes associated with osteoarthritis and pain. Int J Mol Sci, 2014, 15: 14427–14441.
26. Hee HT, Chuah YJ, Tan BH, Setiobudi T, Wong HK. Vascularization and morphological changes of the endplate after axial compression and distraction of the intervertebral disc. Spine (Phila Pa 1976), 2011, 36: 505–511.
27. Ariga K, Yonenobu K, Nakase T, *et al.* Mechanical stress-induced apoptosis of endplate chondrocytes in organ-cultured mouse intervertebral discs: an *ex vivo* study. Spine (Phila Pa 1976), 2003, 28: 1528–1533.
28. Onodera K, Takahashi I, Sasano Y, *et al.* Stepwise mechanical stretching inhibits chondrogenesis through cell-matrix adhesion mediated by integrins in embryonic rat limb-bud mesenchymal cells. Eur J Cell Biol, 2005, 84: 45–58.
29. Xia DD, Lin SL, Wang XY, *et al.* Effects of shear force on intervertebral disc: an in vivo rabbit study. Eur Spine J, 2015, 24: 1711–1719.
30. Inada M, Wang Y, Byrne MH, *et al.* Critical roles for collagenase-3 (Mmp13) in development of growth plate cartilage and in endochondral ossification. Proc Natl Acad Sci U S A, 2004, 101: 17192–17197.